frontiers in Mechanical Engineering

ORIGINAL RESEARCH
published: 19 May 2020
doi: 10.3389/fmech.2020.00026

Experimental Investigation of Performance and Emissions of Ethanol and n-Butanol Fuel Blends in a Heavy-Duty Diesel Engine

Jinlin Han, Weiye He and L. M. T. Somers*

Power & Flow, Department of Mechanical Engineering, Eindhoven University of Technology, Eindhoven, Netherlands

Alcohol fuels are potential alternative fuels for low-temperature combustion concepts in internal combustion engine applications. In this work, 80 vol% of ethanol and 80 vol% of n-butanol are blended with 20 vol% of n-heptane, respectively. These two alcohol fuel blends are investigated in a combustion research unit and a single-cylinder heavy-duty engine to compare the combustion and emission characteristics. The effects of EGR rate and achievable operating load range when using ethanol and n-butanol are the major goals of this investigation. The results show that the ethanol fuel blend requires much higher temperatures to auto-ignite than do the n-butanol blend and diesel. Both alcohol fuel blends show negligible soot emissions in the medium load range when operated with a 40% EGR rate. However, the ethanol fuel blend produces more nucleation mode particles and fewer accumulation mode particles compared to the n-butanol fuel blend under the same operating condition. Furthermore, the particulate size distribution shows that diesel generates more particles with larger particle diameters and thus more soot mass compared to alcohol fuel blends. Still, both alcohol fuel blends can be operated from low to high load with simultaneous reduction of NO_x and soot emissions but at the cost of increased HC and CO emissions. The Euro VI-regulated soot mass and particle number are achieved from low to medium-high load for alcohol fuels. Diesel has the great advantage of achieving high combustion efficiency but shows a NO_x/soot tradeoff at a high EGR rate. Generally, the ethanol fuel blend yields the lowest gross indicated efficiency in the whole test range compared to diesel and the n-butanol fuel blend due to the necessity of inlet heating, which decreases the thermal efficiency. The n-butanol fuel blend achieves the highest gross indicated efficiency (above 50%) in the medium-high load range.

Keywords: emissions, ethanol, n-butanol, efficiency, particle number

OPEN ACCESS

Edited by:
Peng Zhao,
Oakland University, United States

Reviewed by:
Hu Wang,
Tianjin University, China
Alpaslan Atmanli,
National Defense University, Turkey
Dong Han,
Shanghai Jiao Tong University, China

****Correspondence:***
Jinlin Han
j.han.1@tue.nl

Specialty section:
This article was submitted to Engine and Automotive Engineering, a section of the journal Frontiers in Mechanical Engineering

Received: *10 February 2020*
Accepted: *15 April 2020*
Published: *19 May 2020*

Citation:
Han J, He W and Somers LMT (2020) Experimental Investigation of Performance and Emissions of Ethanol and n-Butanol Fuel Blends in a Heavy-Duty Diesel Engine. Front. Mech. Eng. 6:26. doi: 10.3389/fmech.2020.00026

1. INTRODUCTION

The awareness of global warming and greenhouse gas (GHG) emissions gives rise to widespread attention on CO_2 reduction. The European Commission has proposed mandatory regulation of CO_2 for new heavy-duty trucks, suggesting a 15% standard reduction of CO_2 for 2025 and a 30% reduction for 2030, based on the 2019 standard (ICCT, 2018). The agreed-upon targets for light commercial vehicles, meanwhile, aim to reduce the average CO_2 emissions by 15% in 2025 and

by 31% in 2030. Regarding passenger cars, a 15% target for 2025 and a 37.5% target for 2030 were agreed upon, both relative to the 2021 baseline (ICCT, 2019). In addition, increasing worldwide energy demand and concern about the depletion of fossil oil are driving the need for renewable clean energy sources. Among the renewable energy sources, alcohol fuels are often labeled "green" from a life cycle point of view. The CO_2 released from alcohol fuels when used in vehicles can be offset by the CO_2 captured by the crops that are used to produce alcohol fuels. As a result, vehicles running on alcohol fuel blends produce less net CO_2 than conventional fossil fuel vehicles per mile traveled (Wang et al., 2012). Compared to fossil fuel, bio-alcohol fuels can achieve CO_2 reduction potential ranges from 35 to 80% depending on the biomass and process technology used (Schwaderlapp et al., 2012).

Alcohols, such as methanol, ethanol, and butanol are interesting alternative fuels for the low-temperature combustion (LTC) concept due to their high octane number, oxygenated fuel structure, and liquid nature. The application of methanol in internal combustion (IC) engines is plagued by its toxic nature and low energy density (Landälv, 2017). Currently, the major source of methanol is natural gas or coal via gasification followed by methanol synthesis (Sarathy et al., 2014). Hence, biomass-derived ethanol and butanol are more suitable options for application in the IC engine. Both ethanol and butanol can be produced with a variety of technologies and from a number of sources. The first-generation biofuels are derived from food crops, such as cereals, sugar crops, and oilseeds. They have received worldwide criticism due to causing food shortage and competition for land usage (Salehi Jouzani and Taherzadeh, 2015). The second-generation biofuels, however, are mainly obtained from non-edible energy crops, cellulosic waste, agriculture, and forest residues (Parisutham et al., 2014). Both ethanol and butanol are reported to be potential production pathways from this lignocellulosic biomass and woody feedstock (Kumari and Singh, 2018). More recently, ethanol and butanol produced from micro-algae and microbes have started to draw attention. These so-called third and fourth generation biofuels benefit from high photosynthesis and a fast growth rate compared to terrestrial plants (Dutta et al., 2014).

Both ethanol and butanol have been applied and studied in the IC engine due to their favorable chemical and physical properties, with minor modifications to the engine design. Because of its high octane rating and high latent heat of evaporation, ethanol has been applied as an additive or blend-in fuel in the spark-ignition engine and LTC concepts. However, due to its polarized molecular structure, it shows high water affinity, which constrains the mix ratio with gasoline, and it hardly mixes at all with diesel (Sarathy et al., 2014). Shen et al. (2013b) successfully applied pure ethanol in a heavy-duty engine to achieve partially premixed combustion (PPC), with simultaneous Euro VI-compliant soot and NO_x emissions, as well as high thermal efficiency. Ethanol was found to operate in close to stoichiometric (lambda = 1.05) PPC mode with 48.9% of gross indicated efficiency (GIE) and negligible soot emissions at 10 bar gross indicated mean effective pressure (gIMEP). Under the same conditions, diesel and gasoline suffer from high reductions in thermal efficiency and rapid increases in soot emissions (Shen et al., 2013a). Most research has shown a soot mass reduction potential with ethanol fuel blends fuels. When adding 20% ethanol to gasoline, a small PM mass reduction was noticed within test variability, yet when more than 30% ethanol was blended, a 30–46% reduction of PM mass was observed in Maricq et al. (2012). However, the effects of alcohol fuel blends on particle number has not been clearly addressed. In Luo et al. (2015), ethanol-gasoline was reported to increase the particle number (PN) at low load but decrease the PN at high load in a gasoline direct injection (GDI) engine. Storch et al. studied the mixture formation and sooting combustion behavior of E20 (20 vol% of ethanol and 80 vol% of iso-octane) in an optical engine (Storch et al., 2015). The planar laser-induced fluorescence results showed that E20 has a higher sooting tendency compared to iso-octane due to fuel-rich regions with incompletely evaporated fuel droplets remaining from the injection event.

Compared to ethanol, butanol shows superior fuel properties in terms of energy content, lubricity, and corrosivity to metallic construction material (tank, cylinder wall) (Dürre, 2007). Most importantly, butanol is easier to mix with petroleum fuels at a high blend ratio due to its hydrophobicity, and it can be handled by the existing infrastructure (Sarathy et al., 2014). Hence, researchers have shown great interest in butanol both as a component in petroleum fuel and as a self-contained alternative fuel (Atmanli et al., 2015). The combustion and emission characteristics of butanol-diesel fuel blends have been investigated from low to high blend ratio (Valentino et al., 2012; Cheng et al., 2016; Wang et al., 2019). A moderate butanol/diesel mix ratio (50–60%) was concluded to be most optimal for high GIE and low emissions (Leermakers et al., 2013). The addition of butanol to diesel contributes to a more premixed mixture by enlarging the ignition delay and increasing the premixed combustion in the case of both early and late injection timing (Cheng et al., 2014). Soot emissions generally decrease with an increase in the butanol blending ratio. Butanol can influence the cylinder temperature in two counteractive ways: the high latent heat of vaporization decreases the cylinder temperature, while more premixed combustion leads to rapid heat release and a higher combustion temperature. Consequently, the effect of the butanol blending ratio on NO_x is ambiguous and depends on the specific engine and operating conditions (Rajesh Kumar and Saravanan, 2016). However, when a high blend ratio of butanol fuel blend is directly injected into the cylinder, it has adverse consequences, such as a high pressure rise rate (PRR), combustion noise, and limited operating range, particularly when applied in LTC mode (Han et al., 2019). Multiple injection strategies are proposed to stage out the heat release so that maximum pressure rise rate (PRRmax) can be controlled, and both the upper and lower load ranges are extended when a high blend ratio of butanol fuel blends are used (Han et al., 2017, 2018).

These aforementioned studies have shown the merits of applying alcohol fuel blends in IC engines, especially in LTC concepts. However, the particle size concentration distribution in the LTC concept with different alcohol fuels has not been clearly illustrated. Moreover, alcohol fuels would become less attractive if they could only be operated in a very limited

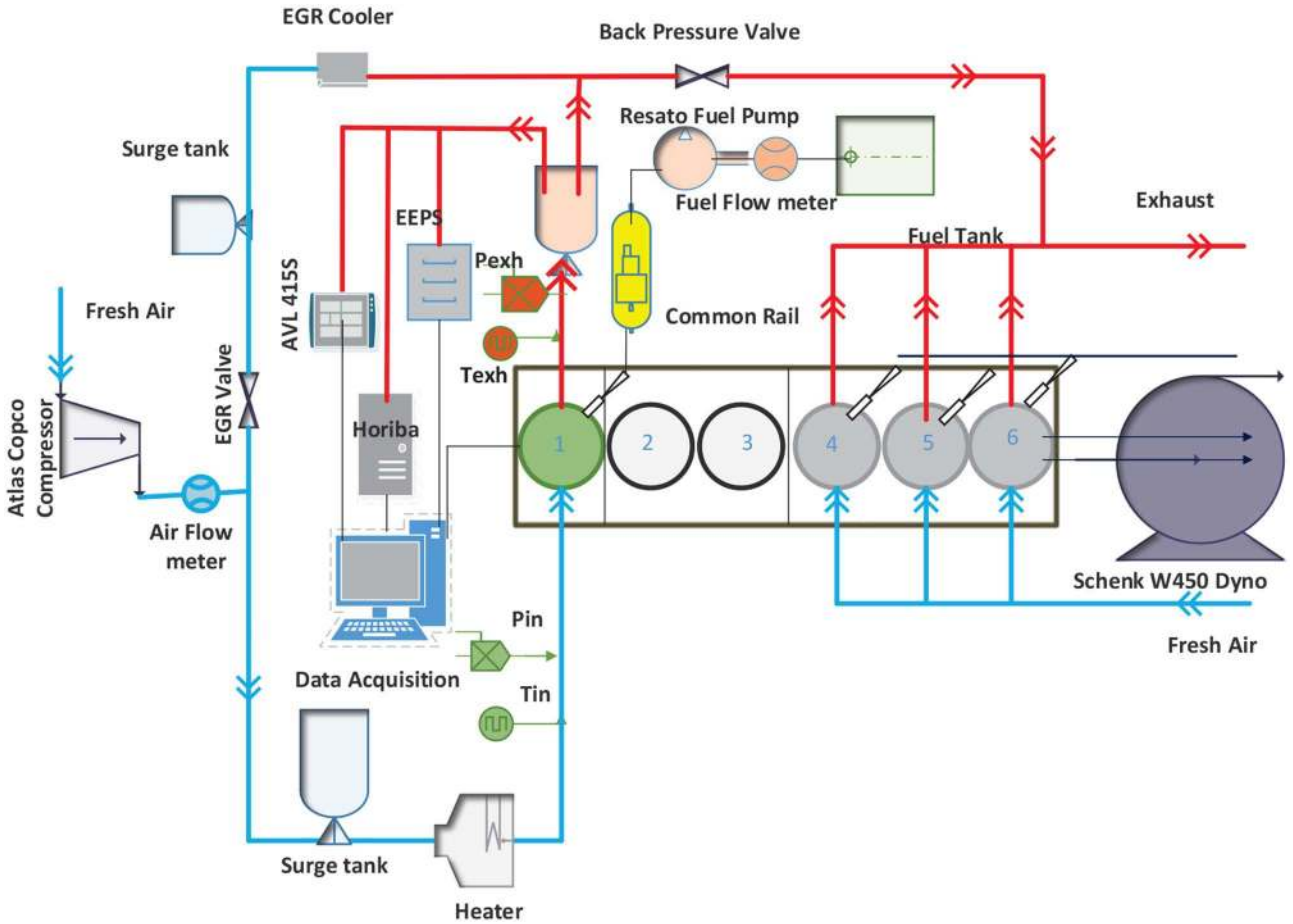

FIGURE 1 | Experimental setup.

operating range compared to petroleum fuels. The operating load range of high-blend-ratio alcohol fuel blends running in LTC has not been fully investigated in the current literature. The main goal of this work is to compare the combustion and emission characteristics of ethanol and n-butanol fuel blends both in a constant volume combustion chamber (CVCC) setup and a diesel engine setup. The particulate size distribution and operating load of alcohol fuels will be evaluated in this paper. Since ethanol cannot homogeneously mix with commercial diesel without an emulsifier or a co-solvent, to make a fair comparison, n-heptane is chosen to replace diesel due to its similar ignition propensity. Particularly, LTC generally necessitates a long ignition delay to promote the mixing between fuel and air and achieve premixed-dominant combustion. Hence, in this work, high alcohol fuel blend ratios are adopted, specifically aiming at a low reactivity: 80 vol% of ethanol and 80 vol% of n-butanol are blended with 20 vol% n-heptane, named EH80 and BH80, respectively. Diesel is tested as the baseline fuel under default calibration except for the exhaust gas recirculation (EGR) rate, which is enhanced to control NO_x emissions. Both BH80 and EH80 are tested with similar operating conditions. A high PRR is a consequence and is actually the limiting factor in these approaches and so is an integral part of the study.

2. APPARATUS AND METHODOLOGY

2.1. Experimental Setup

The combustion research unit (CRU) instrument from FuelTech Solutions is used as an auxiliary setup to both qualitatively and quantitatively study fuel properties. Based on a well-established CVCC technology, the CRU can be set to a specified ambient condition to investigate different fuel characteristics as a function of the process parameters (pressure, temperature, injection pressure, etc.). The ambient conditions are close to the condition in an IC engine, although the maximum temperature is limited to 580°C. Due to the elimination of the engine dynamics (e.g. piston movement), the effects of varying fuel properties and compositions are much easier to isolate and study. The combustion chamber is filled with synthetic air and pure nitrogen. The oxygen concentration can be regulated by the blend ratio of these two gases. Furthermore, it is equipped with an industry-standard common rail injection system. With a flexible modular design, the CRU is built of components and sub-systems

(injection system and optical accessibility) that can be adapted to specific research requirements. More detailed information about the instrument can be found in Solutions (2017).

The experimental engine setup is shown in **Figure 1**. It is modified from an in-stock six-cylinder heavy-duty DAF XE355c engine. Only the first cylinder is the test cylinder and runs with the specific fuel. Cylinders 2 and 3 are disabled. The remaining cylinders propel the engine with diesel to maintain the desired speed with the help of a Schenk W450 hydraulic dynamometer. The test cylinder is isolated from the propelling cylinders except for the crankshaft and camshafts. The inlet pressure is supplied by an external air compressor. Exhaust gas is first cooled and then mixed with fresh air in the surge tank to ensure sufficient mixing. The other two surge tanks are put in place to reduce the pressure oscillation to obtain steady flow. The inlet temperature is controlled by an electrical heater to set the desired inlet condition. A Resato HPU200-625-2 double-acting air-driven pump provides the desired fuel pressure. An accumulator is placed near the fuel injector to simulate the volume of a typical common rail and dampen the pressure fluctuations originating from the fuel pump. Direct injection of the test cylinder is via an injector provided by Delphi. All steady flows of air and fuel are measured with Micro Motion mass flow meters.

Gaseous exhaust emissions are analyzed by a Horiba Mexa 7100 DEGR emission system. The exhaust smoke level in terms of filter smoke number (FSN) is measured by an AVL 415s smoke meter. Particle size concentration and distribution are measured by an engine exhaust particle sizer (TSI EEPS 3090). In this work, the exhaust was sampled at 1 Hz for a period of 1 minute. During the tests, primary dilution was set to a factor of 50 and a temperature of 150°C. The secondary dilution factor and temperature were set at 6.7 and 300°C, respectively. As a result, the total dilution ratio is 335. Inlet pressure and temperature, exhaust pressure and temperature, water and oil temperature are measured by common engine sensors. Data from these sensors, as well as air and fuel flows and emission levels, are recorded at 20 Hz for a period of 40s with an in-house data acquisition system (TueDACs). An AVL GU21C uncooled pressure transducer is flush-mounted in the cylinder and measures in-cylinder pressure at 0.1°CA intervals. In-cylinder pressure, together with crank angle, fuel pressure, and injector current, is recorded and processed by a SMETEC Combi data-acquisition system. Other important test setup parameters are listed in **Table 1**.

TABLE 1 | Engine specification.

Base engine	DAF XE355c
Stroke (mm)	158
Bore (mm)	130
Connecting rod (mm)	266.7
Compression ratio	15.85:1
Number of valves	4
Exhaust valve close (°CA)	−346
Intake valve close (°CA)	−153
Exhaust valve open (°CA)	128
Intake valve open (°CA)	344
Valve overlap (°CA)	30
Injector	Delphi F2P
Actuating type	Solenoid
Nozzle holes	7
Nozzle diameter (mm)	0.195
Included spray angle (°C)	139

TABLE 2 | Properties of fuels.

Fuel	CN	RON	LHV (MJ/kg)	AF_s	Boiling point (K)
Ethanol	–	109	26.8	8.97	351.3
n-Butanol	–	98	33.08	11.13	390.4
n-Heptane	56.3	0	44.5	15.2	371.57
BH80		78.4	35.3	11.85	–
EH80	–	87.2	30.3	10.07	–
EN590	51	–	42.9	14.7	422–644

2.2. Experimental Method

In this paper, the tested ethanol (purity >99.9%), n-butanol (purity >99.5%), and n-heptane (purity >99.75%) are supplied by JBC Solutions. The diesel is EN590. To prevent the injector being damaged due to the low lubricity of alcohol fuels, 0.1 vol% of R655 from Infineum is added to BH80 (80 vol% n-butanol and 20 vol% n-heptane) and EH80 (80 vol% n-butanol and 20 vol% n-heptane). Considering the low concentration of additive, the effects of R655 on the combustion and emission characteristics of alcohol fuel blends are assumed to be negligible. No phase separation is noticed after splash blending and standing for 48 hours for both BH80 and EH80. The major properties of the tested fuels are given in **Table 2**. The LHV and research octane number (RON) of alcohol fuel blends are based on a linear calculation.

In the first part of this work, the effects of chamber temperature and chamber pressure on the ignition quality of alcohol fuels and diesel are compared on the CRU. During the operation, the injection pressure and injection duration are set as 1,500 bar and 1.5 ms, respectively, for all fuels. Fuel is directly injected into the pressurized and heated combustion chamber, where it meets the hot air and ignites. The pressure trace of the combustion chamber after ignition is automatically recorded and saved by the software control system. Chamber temperature is swept from 450 to 575°C in steps of 25°C for BH80 and diesel, while EH80 is only tested at 575 and 580°C. The chamber pressure is swept from 35 to 60 bar in steps of 5 bar for all three fuels.

In the second part of this work, alcohol fuel blends are tested on the heavy-duty engine setup to investigate the load range of alcohol fuels. A double-injection strategy is applied on alcohol fuel blends based on our previous work (Han et al., 2018, 2019), with the first direct injection pulse (DI-1) fixed at −30°CA aTDC. The second injection (DI-2) is close to the top dead center (TDC) and adjusted for proper combustion phasing. The injection duration ratio DI-1/DI-2 is constant at 0.6 ± 0.02. Diesel is also tested to provide a reference. A

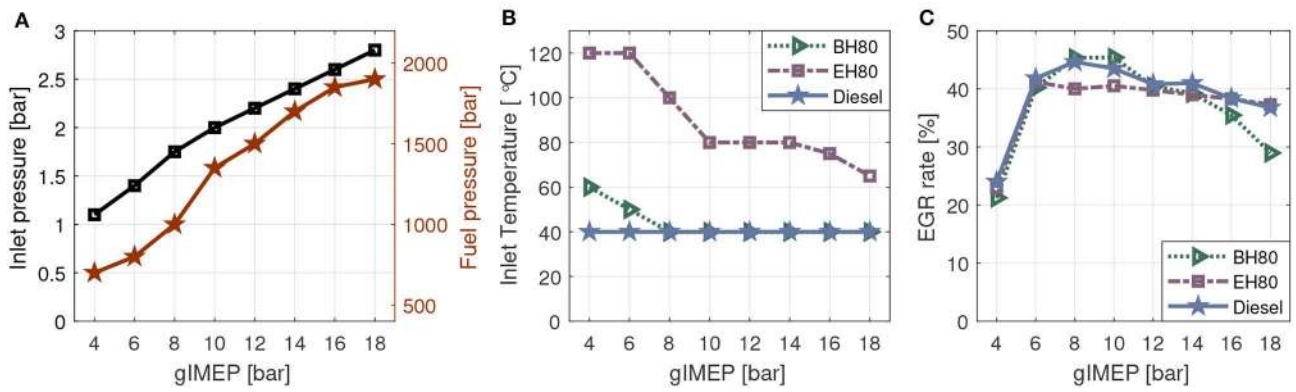

FIGURE 2 | Inlet pressure and fuel pressure vs gIMEP **(A)**, Inlet temperature vs gIMEP **(B)**, and EGR rate vs gIMEP **(C)**.

single injection strategy is used for diesel, wherein the injection timing and the injection duration are adjusted to achieve the desired load and combustion phasing. Diesel operation is set according to the original calibration except for the EGR rate, which is adjusted to control the NO_x emissions. Both alcohol fuel blends and diesel are tested under the same operating conditions with similar combustion phasing from 4 to 18 bar gIMEP in steps of 2 bar. The inlet pressure and injection pressure are the same for both alcohol fuel blends and diesel, as is shown in **Figure 2A**, similar to the original calibration settings of the engine. Since ethanol and n-butanol have much lower reactivity than diesel, compression ignition would be difficult, and misfire tends to happen due to the excessive long ignition delay, especially at low load. Inlet heating is generally applied with alcohol fuel blends to enhance the reactivity of the combustible mixture, and stable combustion can be guaranteed. As is shown in **Figure 2B**, EH80 requires a much higher inlet temperature than BH80 for stable combustion, 120°C is needed at 4 and 6 bar gIMEP. BH80 only requires 60 and 50°C at 4 and 6 bar gIMEP, respectively, and the remaining operating loads are maintained at 40°C, which is the same as diesel. For the same reason, the EGR rate of EH80 cases is restricted to 40% in case of misfire. Considering the lower lubricity of BH80 and EH80, fuel pressure is constrained at 1,950 bar to prevent injector damage. The EGR rate is adjusted to achieve a similar global lambda and simultaneously low NO_x/soot emissions at a specific load, and thus it may vary for different fuels (**Figure 2C**). Additionally, the effects of the EGR rate on EH80 and BH80 are tested in a medium load range (8, 10, and 12 bar gIMEP) to compare the combustion and emission characteristics of ethanol and n-butanol.

2.3. Data Analysis

For CRU tests, each measurement is repeated 10 times and averaged. The ignition delay of CRU is defined as the time interval after injection until a 0.2 bar pressure rise is first reached. For engine tests, each measurement is repeated at least twice. The results are the averaged value of these repetitions. An engine up consists of 70 cycles of in-cylinder pressure traces averaged and filtered using a Savitzky-Golay filter (Order: 1, Frame length: 19). The pressure rise rate is the derivative of the filtered in-cylinder pressure trace per 0.1°CA. gIMEP is calculated from in-cylinder pressure according to Equation (1), where P is the cylinder pressure trace, V is the displacement, and V_d indicates the total stroke volume of the cylinder. The rate of heat release (ROHR) is calculated based on Equation (2) without considering the heat transfer, where θ refers to the crank angle and the specific heat capacity ratio (γ) is based on Equation (3) (Brunt et al., 1998). T is the global temperature calculated from the cylinder pressure based on the ideal gas law. The accumulated heat release can be calculated as the integral of ROHR. Combustion phasing is defined as the crank angle at which 50% heat is released (CA50). Combustion efficiency and gross indicated efficiency are calculated based on Equations (4) and (5). Global lambda is calculated based on the Brettschneider Equation (6) (Torok et al., 2018).

$$gIMEP = \frac{W_{gross}}{V_d} = \frac{\int_{-180}^{180} PdV}{V_d} \tag{1}$$

$$ROHR = \frac{\gamma}{\gamma - 1} P \frac{\partial V}{\partial \theta} + \frac{1}{\gamma - 1} V \frac{\partial P}{\partial \theta} \tag{2}$$

$$\gamma = 1.35 - 6 \times 10^{-5} T + 1 \times 10^{-8} T^2 \tag{3}$$

$$\eta_{Combustion} = \left(1 - \frac{IS_{HC} \times LHV_{fuel} + IS_{CO} \times LHV_{CO} + IS_{H_2} \times LHV_{H_2}}{IS_{FC} \times LHV_{fuel}}\right) \times 100\% \tag{4}$$

where IS_X, IS_{FC}, and LHV are the indicated specific emissions, indicated specific fuel consumption, and lower heating value, respectively.

$$\eta_{GIE} = \frac{\int_{-180}^{180} PdV}{m_{fuel} \times LHV_{fuel}} \times 100\%, \tag{5}$$

where m_{fuel} is the fuel mass per cycle.

$$\lambda = \frac{[CO_2] + [\frac{CO}{2}] + [O_2] + \frac{[NO]}{2} + (\frac{H/C}{4} \times \frac{3.5}{3.5 + \frac{[CO]}{[CO_2]}} - \frac{O/C}{2}) \times ([CO_2] + [CO])}{(1 + \frac{H/C}{4} - \frac{O/C}{2}) \times ([CO_2] + [CO] + (C_n \times [HC]))}. \quad (6)$$

Here, [X] is the exhaust gas volume concentration of compound X, *H/C* and *O/C* are the atom ratios of the fuel, and C_n is the number of carbon atoms in the hydrocarbon molecule.

3. RESULTS AND DISCUSSION

3.1. Ignition Characteristics

Figure 3 shows the ignition quality of the three fuels. The ignition delay period consists of both the physical delay, wherein liquid fuel breaks up into small droplets, atomizes, vaporizes, and entrains ambient air, and the chemical delay contributed by pre-combustion reactions. It can be seen that alcohol fuel blends show a distinctly different ignition propensity from diesel, with a much longer ignition delay observed. At 60 bar chamber pressure, no combustion is observed for EH80 at the maximum available chamber temperature, as is shown in **Figure 4A**. The ignition delay of EH80 is 21.3 ms, even at a chamber temperature of 580°C. For BH80, the ignition delay decreases rapidly with increased chamber temperature. This can be validated by the chamber pressure rise trace (**Figure 4B**): there is barely any pressure rise when the temperature is below 500°C. Proper ignition occurs until the chamber temperature reaches 525°C. The results also indicate that EH80 will require a higher inlet temperature than BH80 in the metal engine experiment. Notably, diesel presents very good ignition quality in the whole test range (**Figure 4C**), and ignition delay decreases as chamber temperature increases (**Figure 3A**).

The observed dependence of ignition propensity on chamber pressure shown in **Figure 3B** can be understood as follows. In a CVCC, high chamber pressure also means higher air mass and ambient density. Thus, the molar concentration of oxygen increases, which shortens the chemical ignition delays. It also leads to a higher entrainment rate such that fuel and oxygen are better mixed, which shortens the physical ignition delay. However, the reaction rate is more influenced by the temperature than by the oxygen molar concentration due to exponential dependence. At 60 bar, the ignition delay of BH80 decreases from 9.83 to 3.29 ms when the chamber temperature is enhanced from 500 to 575°C, whereas the ignition delay of BH80 only decreases from 5.3 to 4.1 ms as the chamber pressure increases from 35 to 60 bar at 550°C. A similar trend can be found for diesel. Therefore, chamber temperature is a more crucial factor in the chamber ambient conditions, especially for low reactivity fuels. In a reciprocating engine, cylinder temperature and cylinder pressure are closely coupled. Inlet pressure boosting can effectively decrease ignition delay since both cylinder pressure and temperature increase after compression. Inlet heating, however, increases the charge temperature but possibly leads to a lower cylinder pressure as a result of decreased charged density (Han et al., 2019).

3.2. Effects of EGR on Alcohol Fuel Blends

The effects of EGR on different alcohol fuel blends will be discussed in this section. For all cases, the DI-1 timing is fixed at −30°CA, which causes fuel injected in DI-1 to be well-mixed with air and contributes to premixed-combustion, whereas, DI-2 behaves like a CDC due to the overlap between the injection and combustion events. As is shown in **Figure 5**, the ROHR profile of DI-2 consists of a premixed peak, a mixing-controlled combustion, and a burn-out. It can be seen that the cylinder pressure peak decreases and the combustion phasing is retarded at a high EGR rate. However, BH80 and EH80 present distinctly different combustion behaviors. At 8-bar gIMEP, BH80 always shows earlier ignition than EH80. As the EGR rate increases, the ROHR profiles of BH80 gradually switch from dual-peak to mono-peak due to the extended mixing time at a high EGR rate, while EH80 remains mono-peaked for all EGR cases. Moreover, BH80 auto-ignites before the second direct injection (DI-2) regardless of the EGR rate at 10 bar and 12 bar. Under these conditions, the reactivity of the combustible mixture increases due to the increased cylinder temperature and oxygen concentration. Specifically, a multi-stage heat release pattern is shown for BH80, which consists of a premixed dominated combustion from DI-1 and a mainly mixing-controlled combustion from DI-2. The two stages of heat release are separated at low EGR rate cases for 10 bar gIMEP and all cases for 12 bar gIMEP. EH80 always presents a mono-peaked ROHR (premixed dominant combustion) at 8 and 10 bar. Additionally, as the ignition delay is elongated at a high EGR rate, more premixed combustion and higher maximum ROHR are observed. At 12 bar gIMEP, EH80 starts to ignite before DI-2 at 25% EGR, and a multi-stage heat release can be noticed, which is similar to BH80. However, the ROHR profile switches to mono-peaked again at 40% EGR. All of these observations of differences between these two alcohol fuel blends are perfectly in line with the difference in octane number of ethanol and n-butanol.

Generally, an increased EGR rate leads to reduced global oxygen availability and temperature, which effectively constrains the formation rate of NO_x emissions, as is shown in **Figure 6A**. A good correlation between NO_x emissions and global temperature can be observed. It is also interesting to find that EH80 generally yields more NO_x emissions than BH80 because of increased bulk temperature. Firstly, EH80 is operated with a higher inlet temperature for all cases, which also leads to a higher bulk temperature as a result of decreased air density and dilution level. Secondly, EH80 presents more premixed combustion phasing, which consequently results in faster heat release and thus higher local temperature than BH80 (**Figure 5**). With a 40% EGR rate, both BH80 and EH80 can achieve engine-out NO_x emissions close to Euro VI-regulated standards. Soot emissions are detected by the AVL 415s smoke meter, which uses the filter paper method to measure the filter smoke number (FSN). The averaged results of three samples of 1L are converted into soot mass by

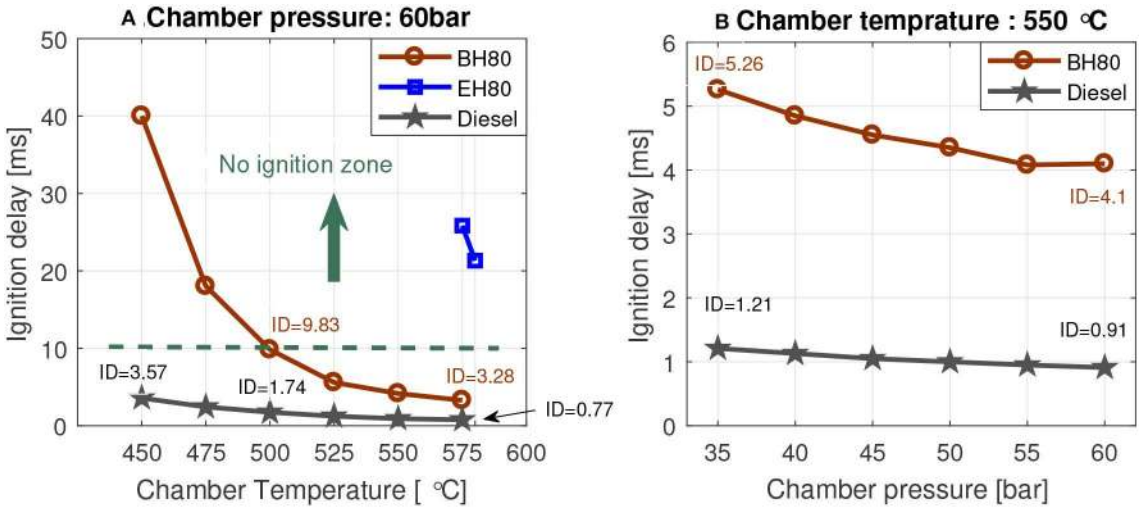

FIGURE 3 | Ignition delay as a function of chamber temperature **(A)** and chamber pressure **(B)**. **(A)** Chamber pressure: 60 bar. **(B)** Chamber temperature: 550°C.

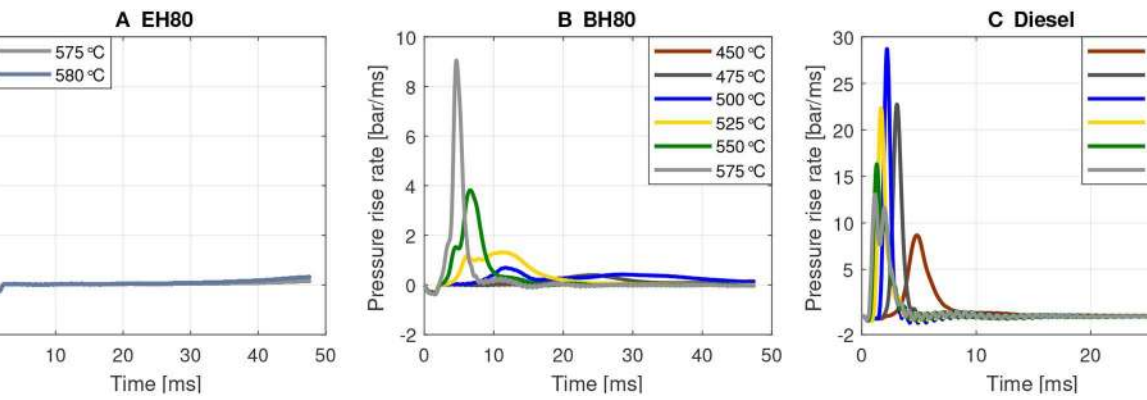

FIGURE 4 | Pressure rise rate at different chamber temperatures. **(A)** EH80. **(B)** BH80. **(C)** Diesel.

the correlation proposed by Northrop et al. (2011). Given the fact that soot oxidation deteriorates at high EGR rates due to decreased oxygen, avoiding the formation of soot is essential to mitigate the NO_x/soot tradeoff when EGR is applied. Alcohol fuel blends benefit from the oxygen atom in the molecule and a longer ignition delay. This avoids the formation of fuel-rich hot areas where soot is produced. As is shown in **Figure 6B**, soot formation is considerably reduced for EH80, since hardly any soot is measured regardless of load and EGR. This holds to a lesser extent for BH80, but it also remains below the Euro VI-regulated soot mass.

It should be noted that these measurements do not indicate particle-free combustion. LTC concepts like homogeneous charge compression ignition (HCCI), PPC, and reactivity controlled compression ignition (RCCI), which apply high EGR rates and high boosting levels, tend to have a longer ignition delay than conventional diesel combustion (CDC) to achieve mostly premixed combustion to reduce soot formation (Musculus et al., 2013). The particle size from LTC generally appears to be smaller than those from CDC, and are particles likely small enough to pass through the filter paper (Prikhodko et al., 2010). Also, small particles only contain 0.1–10% of the total PM mass, so these LTC concepts also yield low soot mass results compared to diesel combustion operated with a high EGR rate. **Figure 6C** shows the particle size distributions of BH80 and EH80 at a 40% EGR rate, which are the worst cases for soot. Both BH80 and EH80 present a bimodal particulate size distribution, which mainly consists of particles in the low end of accumulation mode (20 nm < particle diameter < 100 nm) and a small concentration of nucleation mode particles (particle diameter < 20 nm). Interestingly, EH80 produces fewer accumulation mode particles but more nucleation mode particles under the same operating conditions than does BH80. There are several potential reasons for this. Firstly, as is found that EH80 shows a longer mixing time between fuel and air, which suppresses thermal pyrolysis and dehydrogenation

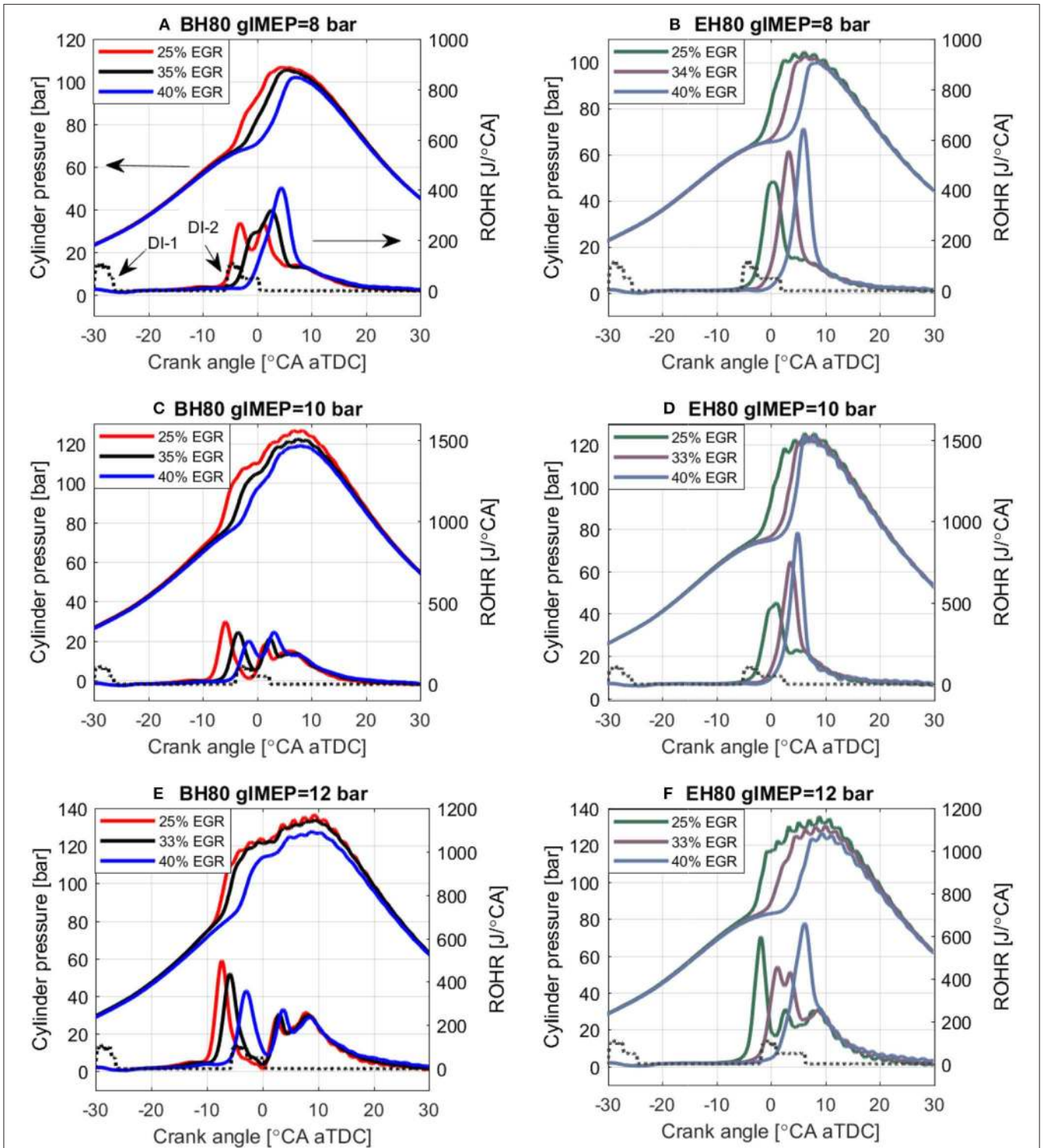

FIGURE 5 | Cylinder pressure and ROHR profiles of EH80 and BH80 at various loads and EGR rates. **(A)** BH80 gIMEP = 8 bar. **(B)** EH80 gIMEP = 8 bar. **(C)** BH80 gIMEP = 10 bar. **(D)** EH80 gIMEP = 10 bar. **(E)** BH80 gIMEP = 12 bar. **(F)** EH80 gIMEP = 12 bar.

reactions. Consequently, the formation of soot-precursor PAHs is constrained. Secondly, EH80 benefits from a higher O/C ratio so that the local equivalence ratio is lower, and the oxidation rate is enhanced (Esarte et al., 2012). Thus, it decreases the reaction rate of particle surface growth by the large hydrocarbons for the accumulation mode particles (Zhang

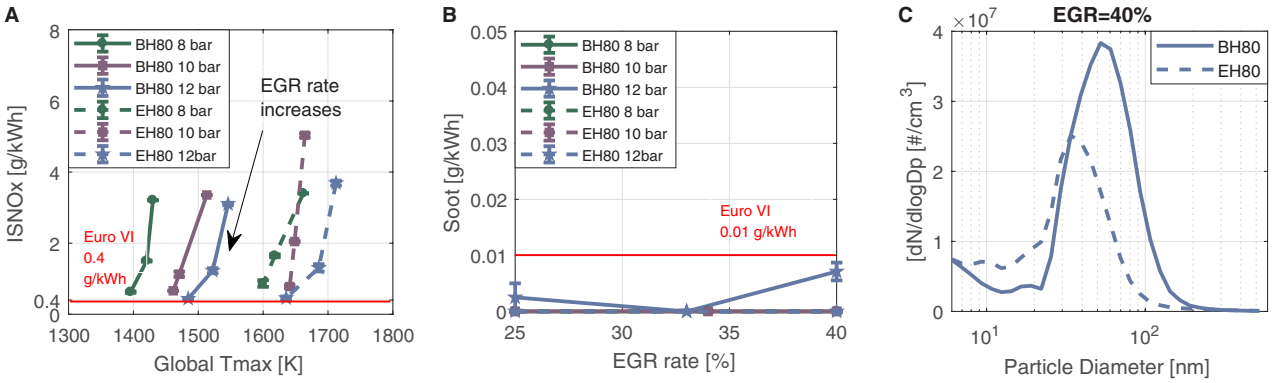

FIGURE 6 | $ISNO_x$ vs. Global Tmax **(A)**, ISPM vs. EGR rate **(B)**, and particle size distribution at a 40% EGR rate **(C)**.

et al., 2014). Simultaneously, since there are fewer accumulation mode particles to absorb the volatile hydrocarbons, these volatile organics are more likely to experience the gas-to-particle process and condense into nucleation mode particles. The results for particle concentration and size distribution confirm the soot mass results. EH80 hardly shows any soot blackening in the filter paper due to the low particle number concentration and small particle size, whereas BH80 shows a much higher concentration of accumulation mode particles at high EGR cases, and hence more soot was measured. The current emission regulations mainly focus on particle mass and total particle number, but there is no particle size and distribution regulation. Caution should be taken when alcohol-blended fuels are applied in a real engine situation since ultrafine particles are dangerous for the human respiratory system (Brown et al., 2002; Labecki et al., 2013). The results presented here are consistent with the results reported in Luo et al. (2015), where the authors showed that the addition of ethanol in gasoline in GDI engines can increase the small particle number and volatile organic compound mass fraction because ethanol inhibits the formation of soot precursors.

3.3. Operating Load Range

In this section, the operating load range of alcohol fuel blends will be discussed. It can be seen from **Figure 7A** that the three tested fuels present similar CA50. CA50 is retarded at high load to prevent excessive peak cylinder pressure and PRRmax. Additionally, the global lambda decreases as the load increases due to increased fueling and limited boosting level in a practical engine. As is shown in **Figure 7B**, both alcohol fuel blends and diesel are set to show identical global lambda by adjusting EGR and boosting the level from 4 to 14 bar gIMEP. In 16 and 18 bar cases, only BH80 shows higher lambda due to the lower EGR rate that needed to be applied.

PRRmax and the coefficient of variance of gIMEP (COV_{gIMEP}) are shown in **Figure 8**. PRRmax is one of the challenges that constrain the operating load range of LTC concepts. It directly reflects the combustion intensity. High PRRmax could result in detrimental consequences like deterioration of engine performance and severe engine noise. As shown in **Figure 8A**, diesel can be operated stably regardless of the operating load. The PRRmax of diesel is much lower than that of alcohol fuel blends, especially at high load cases. Moreover, alcohol fuel blends tend to display a higher PRRmax as the load increases. Notably, BH80 shows lower PRRmax than EH80 up to 14 bar gIMEP, after which PRRmax increases rapidly at 16 and 18 bar. This is mainly caused by the premixed combustion from the DI-1. As mentioned earlier, BH80 presents a two-stage heat release mode. The premixed combustion from DI-1 becomes quite pronounced at 16 and 18 bar gIMEP. Hence, the timing of PRRmax is well before TDC in these high-load cases, as is shown in **Figure 8B**. The location of PRRmax for EH80 and diesel is closer to TDC. This can also be observed in the heat release pattern in **Figure 9**. The phasing of the first stage premixed combustion for BH80 is much earlier than TDC, which causes high pressure rise rates and increased compression work. Additionally, typical mixing-controlled combustion from DI-2 is observed, quite similar to diesel. Even though the three fuels are operated at similar CA50, this early first stage premixed combustion leads to higher peak pressure than for EH80 and diesel. In fact, both the peak pressure and PRRmax limit the high load operation of BH80. Throughout the tested load range, COV_{gIMEP} is quite low, and hardly any fuel-related differences can be found in **Figure 8C**. All three tested fuels show good combustion stability. The general trend shows that COV_{gIMEP} increases at low load, which is because the combustion process in the lean mixture at these low loads becomes more sensitive to small changes (Maurya and Agarwal, 2011).

Figure 10 shows the regulated emissions of the tested fuels. Though diesel manages to decrease the NO_x emissions to quite close to the Euro VI standard at a high EGR rate, the reduction of NO_x comes at the price of high soot emissions. The alcohol fuel blends, however, show great advantages in relieving the NO_x/soot tradeoff. Both BH80 and EH80 have NO_x emissions that are comparable with diesel but much lower soot emissions. Specifically, BH80 achieves a soot mass below the Euro VI standard from 4 to 16 bar gIMEP, 0.03 g/kWh soot emissions are achieved at 18 bar gIMEP. For EH80, negligible soot emissions can be seen from 4 to 14 bar gIMEP, whereas 0.03 and 0.1 g/kWh of soot are achieved at 16 and 18 bar. The higher soot emissions of EH80 at

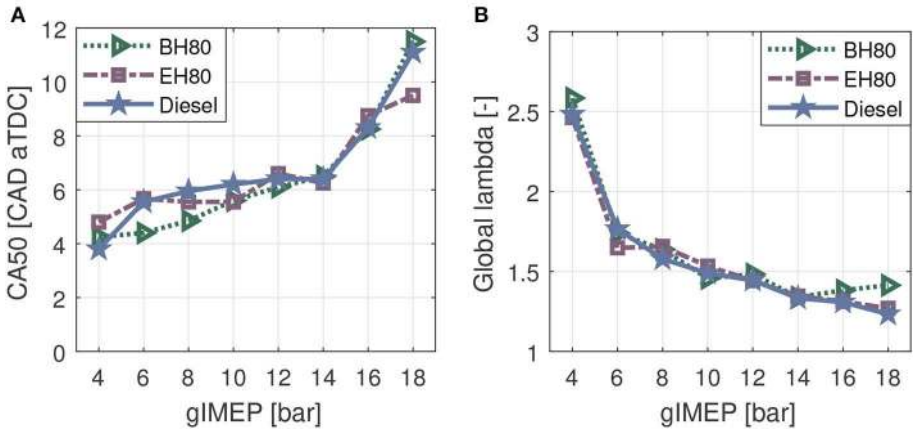

FIGURE 7 | CA50 **(A)** and global lambda **(B)** as a function gIMEP.

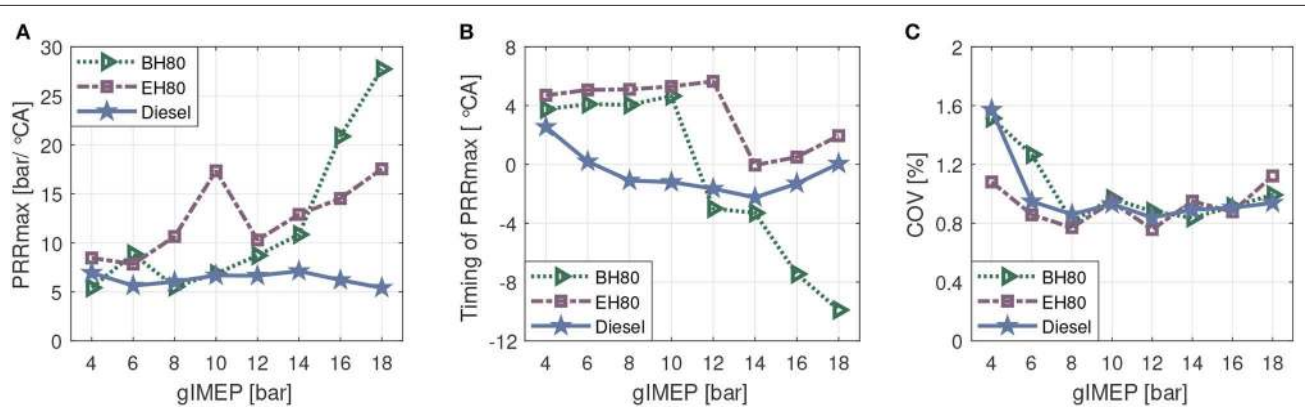

FIGURE 8 | PRRmax **(A)**, Timing of PRPmax **(B)**, and COV_{gIMEP} **(C)** as a function of gIMEP.

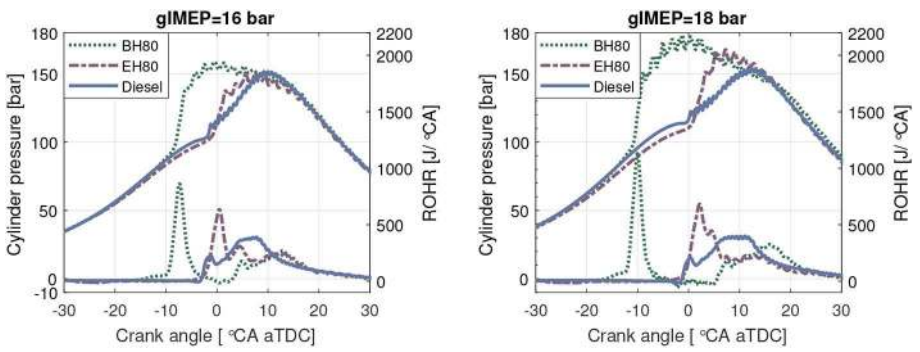

FIGURE 9 | Cylinder-pressure and ROHR at 16 and 18 bar gIMEP.

high load cases compared to BH80 is mainly because of the higher EGR rate that could be applied to constrain the NO_x emissions. This also explains why EH80 displays lower NO_x emissions than BH80 at 16 and 18 bar. The increased soot emissions at high load are expected and are due to the limitations of injection pressure and intake boosting pressure. The global lambda decreases at high load, as shown in **Figure 7**. Therefore, the soot emissions are mostly influenced by ambient oxygen availability since overlap between injection and combustion always exists due to an elongated injection

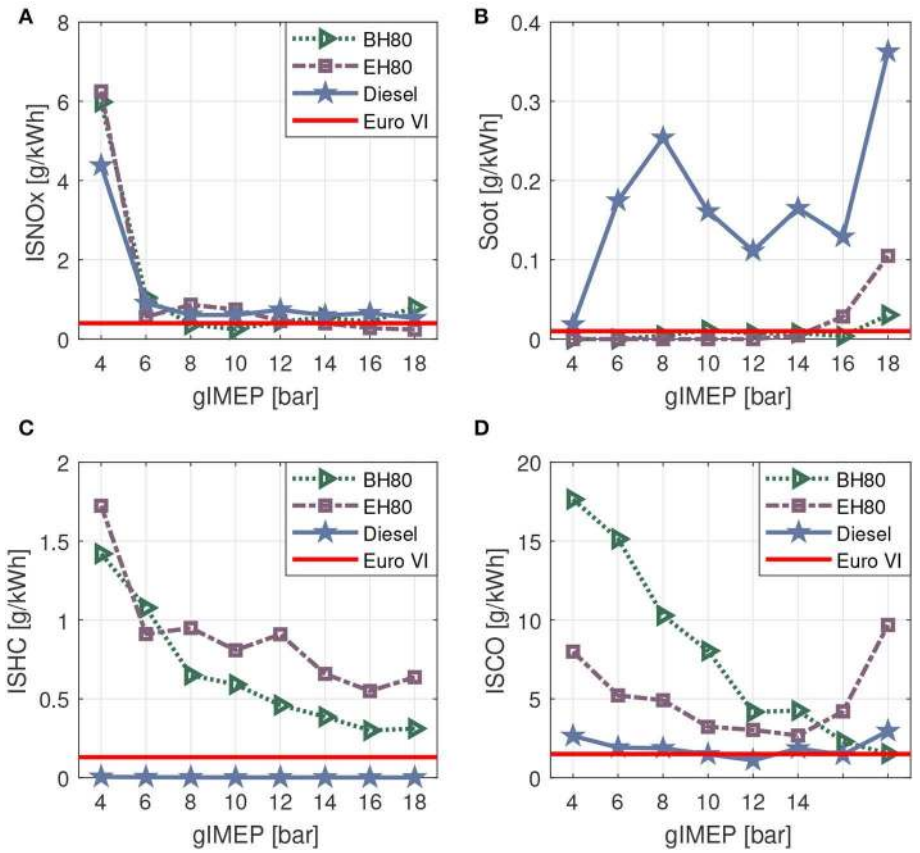

FIGURE 10 | ISNOx **(A)**, Soot **(B)**, ISHC **(C)**, and ISCO **(D)** as a function of gIMEP.

duration at these high load conditions. The irregularity in the soot behavior of diesel cases illustrates that dedicated calibration is necessary when diesel is operated at high EGR rates. **Figures 11A,B** show particle size distribution concentration at 16 and 18 bar gIMEP. All tested fuels present a unimodal distribution of accumulation mode particles. Both particle number concentration and particle diameter increase as the load increase. Compared with diesel, alcohol fuel blends not only yield lower particle number concentrations but also a smaller particle diameter, which is consistent with the soot mass results. This can be mainly attributed to the better mixing between alcohol fuel and air and lower local equivalence ratio due to the oxygenated fuel molecule. In addition, diesel contains aromatic hydrocarbons, which are generally accepted to show the highest soot formation tendency, while EH80 and BH80 mainly consist of alcohol, which is deemed to show the lowest soot formation tendency (Ladommatos et al., 1996). As a consequence, alcohol fuel blends also achieve Euro VI (8×10^{11} 1/kWh)-compliant total particle numbers in the whole operating load range, as shown in **Figure 11C**. Considering that diesel generates a much higher total particle number than alcohol fuel blends, this value for diesel is not shown in the figure for the sake of data clarity.

Generally, LTC concepts feature a long ignition delay so that the fuel and air are better premixed than in CDC. The avoidance of hot fuel-rich areas can mitigate the NO_x/soot tradeoff to some extent. However, the usage of low reactivity fuel generally brings high HC and CO emissions. As is shown in **Figures 10C,D**, both alcohol fuel blends produce more HC and CO emissions than does diesel. It is interesting to note that BH80 yields less HC emissions but more CO emissions compared to EH80, although both HC and CO are products of incomplete combustion. HC emissions are mainly unburned fuel remaining in the crevice volume where flame cannot penetrate because of poor targeting of the injection (Heywood, 1988). However, over-leaning of the mixture due to a long ignition delay is also one of the most common sources of unburned HC emissions from LTC concepts (Opat et al., 2007; Han et al., 2012). EH80 shows longer ignition delay and mixing time compared to BH80, and consequently, the local equivalence ratio is expected to be lower than that of BH80, leading to more HC emissions. As for BH80, it presents more mixing-controlled combustion and, therein, a higher local equivalence ratio area, which promotes the formation rate of CO. Both HC and CO emissions generally decrease at high load due to the increased cylinder temperature. The sudden increase of CO emissions from EH80 at 16 bar

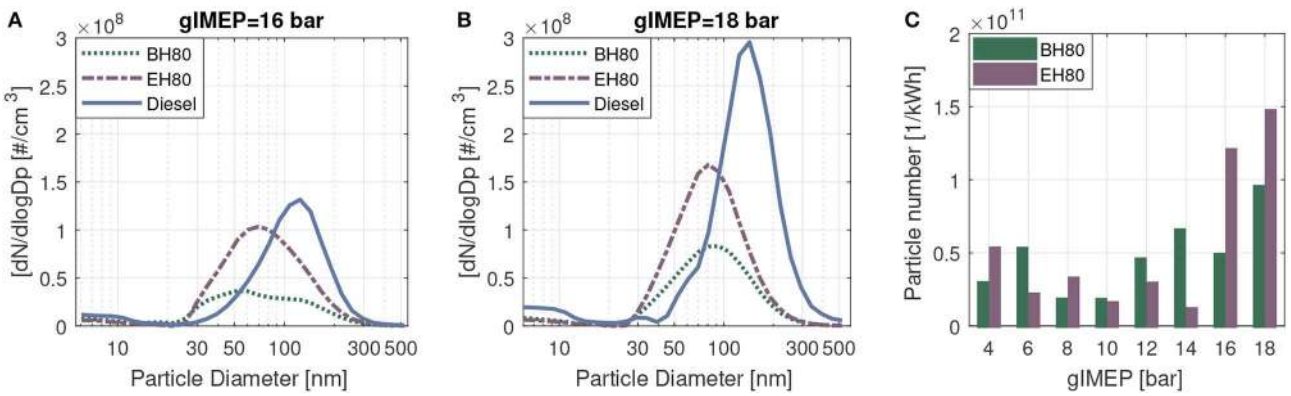

FIGURE 11 | Particle size concentration distribution **(A)** gIMEP = 16 bar, **(B)** gIMEP = 18 bar, and total particle number **(C)**.

and 18 bar can be attributed to the decreased inlet heating temperature, which deteriorates the combustion completeness. Furthermore, since the EGR rate for EH80 is higher than that of BH80 in these two load cases, the lower global lambda also enhances the production of CO emissions. Diesel is injected late, and this avoids the poor targeting. It presents mixing-controlled combustion because of a short ignition delay, and most CO formed in the diffusion flame can be oxidized to CO_2 during the adequately long late combustion stage. It can be seen from **Figure 10C** that diesel shows negligible HC emissions throughout the testing load and Euro VI compliant CO emissions under most operating loads. The results actually demonstrate that the NO_x/soot tradeoff for diesel is replaced by the NO_x-HC/CO tradeoff for the alcohol fuel blends. However, compared to NO_x and soot emissions, HC and CO emissions are much easier and less costly to mitigate by applying a diesel oxidation catalyst (DOC).

Obviously, the high HC/CO emissions are equivalent to low combustion completeness. This reflects directly in the combustion efficiency, as shown in **Figure 12A**. Both BH80 and EH80 have a low combustion efficiency at low load, when the long ignition delay and lower cylinder temperature degrade the combustion completeness. The fact that EH80 outperforms BH80 is due to inlet heating. This helps to stabilize the combustion and reduce the HC and CO emissions. For the same reason, heat transfer loss for EH80 is expected to be larger than that for BH80 and diesel. Combustion efficiency increases at higher loads for both EH80 and BH80. The combustion efficiency of BH80 is close to that of diesel at 16 and 18 bar gIMEP, as it approaches mixing-controlled combustion at these load cases. But even with this lower combustion efficiency, the GIE appears to be promising (**Figure 12B**). BH80 shows higher GIE than diesel from 4 bar to 14 bar. Specifically, more than 50% GIE is achieved from 8 to 14 bar gIMEP. It then decreases due to the enhanced negative compression work caused by the early ignition of DI-1 before TDC. This can be optimized by reducing the injection duration ratio of DI-1/DI-2 so that more work can be extracted in the expansion stroke. For EH80, inlet heating is applied in the whole load range to keep stable combustion, which also decreases the thermal efficiency.

In order to address the efficiency difference in detail, an energy balance analysis was performed, as shown in **Figure 13**. It can be clearly seen that heat transfer loss is the leading reason for the low GIE for EH80. The application of inlet heating is beneficial for reducing combustion loss and maintaining a stable combustion process. However, it also decreases the amount of fresh air charge in the cylinder at a fixed inlet pressure and increases the charge temperature, both of which contribute to a higher combustion temperature and thus higher heat transfer to the wall. Furthermore, the reduced specific heat capacity ratio at high inlet temperature also leads to a decreased thermal efficiency (Lam et al., 2018). In contrast, BH80 benefits from lower heat transfer loss owing to the staged heat release pattern, which lowers the combustion temperature.

4. SUMMARY/CONCLUSIONS

In this work, the combustion and emission characteristics of different alcohol fuel blends are investigated in both CRU and heavy-duty engine setups. Specifically, the effects of EGR rate on high-blend-ratio alcohol fuel blends and the operating load range of alcohol fuel blends are compared with the case of diesel. Based on the experimental results, the following conclusions can be drawn:

1. Alcohol fuel blends show much longer ignition delay than does diesel in both setups. Ambient temperature is much more influential than ambient pressure on the ignition propensity of alcohol fuel blends. BH80 mostly presents two-stage heat release, while EH80 presents premixed dominant combustion. Moreover, EH80 generates more particles in nucleation mode and fewer particles in accumulation mode under the same operating condition.
2. Both EH80 and BH80 can be operated from 4 to 18 bar gIMEP. However, EH80 requires a high inlet temperature (120°C at 4 and 6 bar gIMEP) to maintain stable combustion

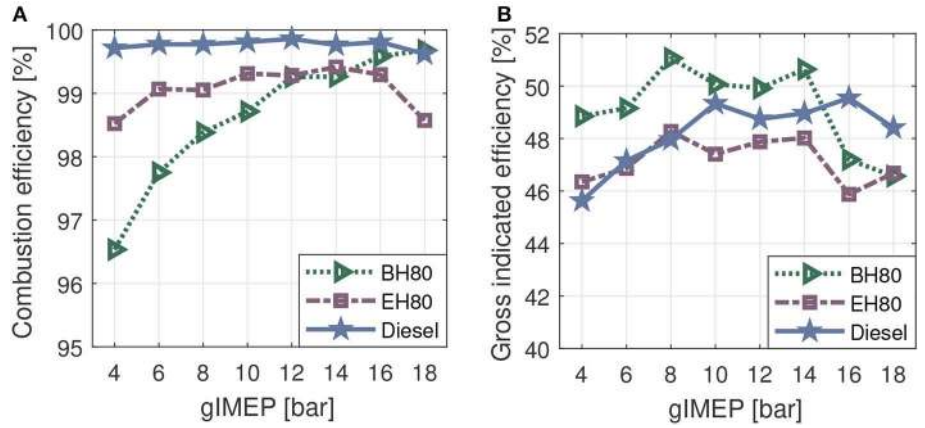

FIGURE 12 | Combustion efficiency **(A)** and gross indicated efficiency **(B)** as a function of gIMEP.

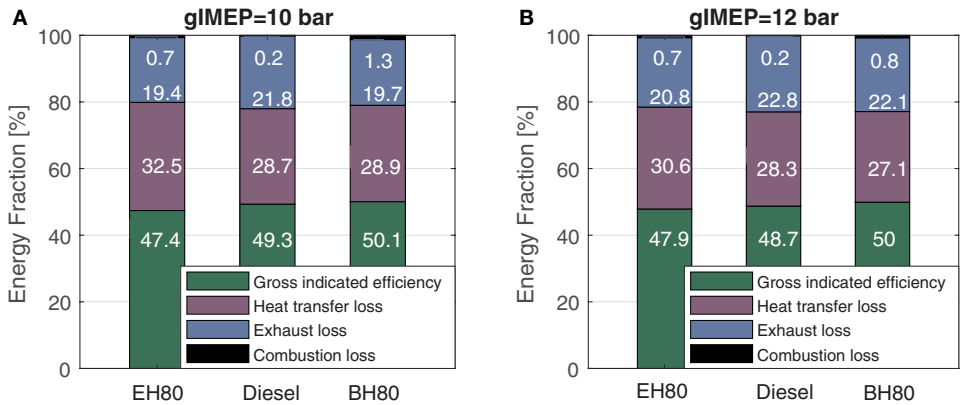

FIGURE 13 | Energy balance analysis. **(A)** gIMEP = 10 bar. **(B)** gIMEP = 12 bar.

in the whole operating range due to its high octane rating, while BH80 only needs moderate inlet temperature at low-load cases (60°C at 4 bar gIMEP and 50°C 6 bar gIMEP).

3. With the help of EGR, all tested fuels show low NO_x emissions from 6 to 18 bar. Diesel shows significantly higher soot mass and larger particle concentration in accumulation mode than the alcohol fuel blends. For alcohol fuel blends, negligible soot mass emissions are observed, and the NO_x/soot tradeoff is mitigated at the cost of increased HC and CO emissions. Specifically, BH80 and EH80 achieve particle mass and particle number below Euro VI regulations from 4 to 14 bar gIMEP.
4. Alcohol fuel blends suffer from combustion incompleteness and thus low combustion efficiency. For EH80, inlet heating also leads to more heat transfer loss, which decreases the GIE in the whole operating range, while BH80 presents a higher GIE than diesel from low to medium-high load. Over 50% GIE is achieved from 8 to 14 bar gIMEP. At high load, GIE decreases mainly because of the increased compression work due to the early ignition of DI-1.

To sum up, bio-alcohols are potential alternative fuels applicable in the LTC concepts. Compared to diesel operation, alcohol fuel blends can mitigate the engine-out NO_x/soot tradeoff at the cost of high HC and CO emissions at low load. High load cases are mainly limited by high PRRmax and peak cylinder pressure due to early premixed-combustion. Particularly, BH80 presents the highest GIE from 4 to 14 bar gIMEP without the need for a high inlet temperature. These promising results illustrate the good performance of bio-alcohol, a fuel that can be derived from an abundant resource (seaweed), in HD diesel engine in a wide operating load range. Future work will focus on the cold flow properties of alcohol fuel blends, the spray and combustion interaction (spray penetration, liquid length, lift-off length, etc.) of alcohol fuel blends in a more advanced setup (an Eindhoven high-pressure cell) with excellent optical accessibility. For the metal engine work, the DI-1/DI-2 ratio will be reduced for high load cases to decrease the PRRmax and further enhance the thermal efficiency (less negative compression work). Moreover, the conversion efficiency of DOC when operated with alcohol fuel blends will be evaluated.

DATA AVAILABILITY STATEMENT

The datasets generated for this study are available on request to the corresponding author.

AUTHOR CONTRIBUTIONS

JH conceived the presented idea, carried out the engine, and took the lead in writing the manuscript. WH carried out the CRU tests under the supervision of JH. The post-processing and data analysis were mainly performed by JH under the supervision of LS. LS provided the critical feedback and helped shape the research, analysis, and manuscript. WH and LS contributed to the final version of the manuscript.

ACKNOWLEDGMENTS

The authors would like to thank Dr. Michel Cuijpers, Guus Dongen, and Bart Pinxton in the Power & Flow group of Eindhoven University of Technology for their valuable contributions in keeping the experimental setups in good condition.

REFERENCES

Atmanli, A., Ileri, E., Yuksel, B., and Yilmaz, N. (2015). Extensive analyses of diesel-vegetable oil-n-butanol ternary blends in a diesel engine. *Appl. Energy* 145, 155–162. doi: 10.1016/j.apenergy.2015.01.071

Brown, J. S., Zeman, K. L., and Bennett, W. D. (2002). Ultrafine particle deposition and clearance in the healthy and obstructed lung. *Am. J. Respir. Crit. Care Med.* 166, 1240–1247. doi: 10.1164/rccm.200205-399OC

Brunt, M. F., Rai, H., and Emtage, A. L. (1998). The calculation of heat release energy from engine cylinder pressure data. *SAE Trans.* 107, 1596–1609. doi: 10.4271/981052

Cheng, X., Li, S., Yang, J., and Liu, B. (2016). Investigation into partially premixed combustion fueled with n-butanol-diesel blends. *Renew. Energy* 86, 723–732. doi: 10.1016/j.renene.2015.08.067

Cheng, X., Shuai, L., Yang, J., Dong, S., and Bao, Z. (2014). *Effect of n-Butanol-Diesel Blends on Partially Premixed Combustion and Emission Characteristics in a Light-Duty Engine*. Technical report, SAE Technical Paper. doi: 10.4271/2014-01-2675

Dürre, P. (2007). Biobutanol: an attractive biofuel. *Biotechnol. J. Healthc. Nutr. Technol.* 2, 1525–1534. doi: 10.1002/biot.200700168

Dutta, K., Daverey, A., and Lin, J.-G. (2014). Evolution retrospective for alternative fuels: first to fourth generation. *Renew. Energy* 69, 114–122. doi: 10.1016/j.renene.2014.02.044

Esarte, C., Abián, M., Millera, Á., Bilbao, R., and Alzueta, M. U. (2012). Gas and soot products formed in the pyrolysis of acetylene mixed with methanol, ethanol, isopropanol or n-butanol. *Energy* 43, 37–46. doi: 10.1016/j.energy.2011.11.027

Han, D., Ickes, A. M., Bohac, S. V., Huang, Z., and Assanis, D. N. (2012). HC and CO emissions of premixed low-temperature combustion fueled by blends of diesel and gasoline. *Fuel* 99, 13–19. doi: 10.1016/j.fuel.2012.04.010

Han, J., Wang, S., and Somers, B. (2018). *Effects of Different Injection Strategies and EGR on Partially Premixed Combustion*. Technical report, SAE Technical Paper. doi: 10.4271/2018-01-1798

Han, J., Wang, S., and Somers, B. (2019). *Comparative Study on the Effects of Inlet Heating, Inlet Boosting, and Double-Injection Strategy on Partially Premixed Combustion*. Technical report, SAE Technical Paper. doi: 10.4271/2019-01-1149

Han, X., Yang, Z., Wang, M., Tjong, J., and Zheng, M. (2017). Clean combustion of n-butanol as a next generation biofuel for diesel engines. *Appl. Energy* 198, 347–359. doi: 10.1016/j.apenergy.2016.12.059

Heywood, J. B. (1988). *Combustion Engine Fundamentals, 1^a edn*. Estados Unidos.

ICCT (2018). *The EU Must Go Further on CO_2 Truck Targets*. ICCT.

ICCT (2019). *CO_2 Emission Standards for Passenger Cars and Light-Commercial Vehicles in the European Union*. ICCT.

Kumari, D., and Singh, R. (2018). Pretreatment of lignocellulosic wastes for biofuel production: a critical review. *Renew. Sustain. Energy Rev.* 90, 877–891. doi: 10.1016/j.rser.2018.03.111

Labecki, L., Lindner, A., Winklmayr, W., Uitz, R., Cracknell, R., and Ganippa, L. (2013). Effects of injection parameters and EGR on exhaust soot particle number-size distribution for diesel and RME fuels in HSDI engines. *Fuel* 112, 224–235. doi: 10.1016/j.fuel.2013.05.013

Ladommatos, N., Rubenstein, P., and Bennett, P. (1996). Some effects of molecular structure of single hydrocarbons on sooting tendency. *Fuel* 75, 114–124. doi: 10.1016/0016-2361(94)00251-7

Lam, N., Tunestal, P., and Andersson, A. (2018). *Analyzing Factors Affecting Gross Indicated Efficiency When Inlet Temperature Is Changed*. Technical report, SAE Technical Paper. doi: 10.4271/2018-01-1780

Landälv, I. (2017). *Methanol as a Renewable Fuel - A Knowledge Synthesis. Report No 2015:08f3.* The Swedish Knowledge Centre for Renewable Transportation Fuels. Available online at: www.f3centre.se

Leermakers, C., Bakker, P., Somers, L., De Goey, L., and Johansson, B. (2013). Butanol-diesel blends for partially premixed combustion. *SAE Int. J. Fuels Lubric.* 6, 217–229. doi: 10.4271/2013-01-1683

Luo, Y., Zhu, L., Fang, J., Zhuang, Z., Guan, C., Xia, C., et al. (2015). Size distribution, chemical composition and oxidation reactivity of particulate matter from gasoline direct injection (GDI) engine fueled with ethanol-gasoline fuel. *Appl. Thermal Eng.* 89, 647–655. doi: 10.1016/j.applthermaleng.2015.06.060

Maricq, M. M., Szente, J. J., and Jahr, K. (2012). The impact of ethanol fuel blends on PM emissions from a light-duty gdi vehicle. *Aerosol Sci. Technol.* 46, 576–583. doi: 10.1080/02786826.2011.648780

Maurya, R. K., and Agarwal, A. K. (2011). Experimental investigation on the effect of intake air temperature and air-fuel ratio on cycle-to-cycle variations of hcci combustion and performance parameters. *Appl. Energy* 88, 1153–1163. doi: 10.1016/j.apenergy.2010.09.027

Musculus, M. P., Miles, P. C., and Pickett, L. M. (2013). Conceptual models for partially premixed low-temperature diesel combustion. *Prog. Energy Combust. Sci.* 39, 246–283. doi: 10.1016/j.pecs.2012.09.001

Northrop, W. F., Bohac, S. V., Chin, J.-Y., and Assanis, D. N. (2011). Comparison of filter smoke number and elemental carbon mass from partially premixed low temperature combustion in a direct-injection diesel engine. *J. Eng. Gas Turbines Power* 133:102804. doi: 10.1115/1.4002918

Opat, R., Ra, Y., Krieger, R., Reitz, R. D., Foster, D. E., Durrett, R. P., et al. (2007). *Investigation of Mixing and Temperature Effects on HC/CO Emissions for Highly Dilute Low Temperature Combustion in a Light Duty Diesel Engine*. Technical report, SAE Technical Paper. doi: 10.4271/2007-01-0193

Parisutham, V., Kim, T. H., and Lee, S. K. (2014). Feasibilities of consolidated bioprocessing microbes: from pretreatment to biofuel production. *Bioresour. Technol.* 161, 431–440. doi: 10.1016/j.biortech.2014.03.114

Prikhodko, V. Y., Curran, S. J., Barone, T. L., Lewis, S. A., Storey, J. M., Cho, K., et al. (2010). Emission characteristics of a diesel engine operating with in-cylinder gasoline and diesel fuel blending. *SAE Int. J. Fuels Lubric.* 3, 946–955. doi: 10.4271/2010-01-2266

Rajesh Kumar, B., and Saravanan, S. (2016). Effect of iso-butanol addition to diesel fuel on performance and emissions of a DI diesel engine with exhaust gas recirculation. *Proc. Inst. Mech. Eng. A J. Power Energy* 230, 112–125. doi: 10.1177/0957650915617107

Salehi Jouzani, G., and Taherzadeh, M. J. (2015). Advances in consolidated bioprocessing systems for bioethanol and butanol production from biomass: a comprehensive review. *Biofuel Res. J.* 2, 152–195. doi: 10.18331/BRJ2015.2.1.4

Sarathy, S. M., Oßwald, P., Hansen, N., and Kohse-Höinghaus, K. (2014). Alcohol combustion chemistry. *Prog. Energy Combust. Sci.* 44, 40–102. doi: 10.1016/j.pecs.2014.04.003

Schwaderlapp, M., Adomeit, P., Kolbeck, A., and Thewes, M. (2012). Ethanol and its potential for downsized engine concepts. *Auto Tech Rev*. 1, 48–53. doi: 10.1365/s40112-012-0022-z

Shen, M., Tuner, M., and Johansson, B. (2013a). *Close to Stoichiometric Partially Premixed Combustion–The Benefit of Ethanol in Comparison to Conventional Fuels*. Technical report, SAE Technical Paper. doi: 10.4271/2013-01-0277

Shen, M., Tuner, M., Johansson, B., and Cannella, W. (2013b). *Effects of EGR and Intake Pressure on PPC of Conventional Diesel, Gasoline and Ethanol in a Heavy Duty Diesel Engine*. Technical report, SAE Technical Paper. doi: 10.4271/2013-01-2702

Solutions, F. (2017). *Service & Maintenance Manual 5.06 CRU*. FuelTech Solutions.

Storch, M., Hinrichsen, F., Wensing, M., Will, S., and Zigan, L. (2015). The effect of ethanol blending on mixture formation, combustion and soot emission studied in an optical DISI engine. *Appl. Energy* 156, 783–792. doi: 10.1016/j.apenergy.2015.06.030

Torok, A., Zoldy, M., and Csefalvay, E. (2018). Effects of renewable energy sources on air-fuel ratio. *J. KONES* 25.

Valentino, G., Corcione, F. E., Iannuzzi, S. E., and Serra, S. (2012). Experimental study on performance and emissions of a high speed diesel engine fuelled with n-butanol diesel blends under premixed low temperature combustion. *Fuel* 92, 295–307. doi: 10.1016/j.fuel.2011.07.035

Wang, M., Han, J., Dunn, J. B., Cai, H., and Elgowainy, A. (2012). Well-to-wheels energy use and greenhouse gas emissions of ethanol from corn, sugarcane and cellulosic biomass for us use. *Environ. Res. Lett*. 7:045905. doi: 10.1088/1748-9326/7/4/045905

Wang, S., Han, J., and Somers, B. (2019). *Performance and Emission Studies in a Heavy-Duty Diesel Engine Fueled With an n-Butanol and n-Heptane Blend*. Technical report, SAE Technical Paper. doi: 10.4271/2019-01-0575

Zhang, Z., Wang, T., Jia, M., Wei, Q., Meng, X., and Shu, G. (2014). Combustion and particle number emissions of a direct injection spark ignition engine operating on ethanol/gasoline and n-butanol/gasoline blends with exhaust gas recirculation. *Fuel* 130, 177–188. doi: 10.1016/j.fuel.2014.04.052

Conflict of Interest: The authors declare that the research was conducted in the absence of any commercial or financial relationships that could be construed as a potential conflict of interest.

NOMENCLATURE

aTDC	After top dead center
BH80	80 vol% n-butanol and 20 vol% n-heptane
BDC	Bottom dead center
CA	Crank angle
CA50	Crank angle at which 50% of heat is released
CDC	Conventional diesel combustion
CN	Cetane number
CO	Carbon monoxide
CO_2	Carbon dioxide
COV	Coefficient of variance
COV_{gIMEP}	Coefficient of variance based on gIMEP
CR	Compression ratio
CRU	Combustion research unit
CVCC	Constant volume combustion chamber
DI	Direct injection
DOC	Diesel oxidation catytist
DI	Direct injection
DI-1	First direct injection
DI-2	Second direct injection
EGR	Exhaust gas recirculation
EH80	80vol% ethanol and 20vol% n-heptane
EOI	End of injection
EVC	Exhaust valve close
EVO	Exhaust valve open
FSN	Filter smoke number
GHG	Greenhouse gas
GIE	Gross indicated efficiency
gIMEP	Gross indicated mean effective pressure
HC	Hydrocarbons
HCCI	Homogeneous charge compression ignition
IC	Internal combustion
IVC	Intake valve close
IVO	Intake valve open
LHV	Lower heating value
LTC	Low temperature combustion
NO_x	Nitrogen oxides
PM	Particulate matter
PN	Particle number
PPC	Partially premixed combustion
PRR	Pressure rise rate
PRRmax	Maximum pressure rise rate
ROHR	Rate of heat release
RON	Research octane number
RPM	Revolutions per minute
SOI	Start of injection
TDC	Top dead center